Duncan, R. A., Backman, J., Peterson, L. C., et al., 1990
Proceedings of the Ocean Drilling Program, Scientific Results, Vol. 115

38. GEOCHEMISTRY AND ORIGIN OF NEOGENE SEDIMENTS IN HOLE 711A[1]

Kurt Boström[2] and Jan Backman[2]

ABSTRACT

Pelagic sedimentation in the northwest Indian Ocean has been studied using sediments from Hole 711A (the section from 0 to 70.5 mbsf, 0–22 Ma), a deep site (4428 m) drilled during Ocean Drilling Program Leg 115. The clay fraction of the sediments represents poorly developed pelagic deposits with considerably lower contents of Mn, Ba, Cu, Ni, Cr, and Zn than is typical for well-oxidized pelagic sediments formed far from the continents (e.g., in the central Indian or Pacific oceans).

Geochemical provenance models, representing conservative mixing models with terrigenous, exhalative-volcanic, and biogenous matter as the only inputs, explain most of the compositional variations in the sediments. The models show that terrigenous matter accounts for about 96%–100% of all SiO_2, Al_2O_3, TiO_2, and Zr; about 73%–85% of all Fe_2O_3, V, and Ni; and about 40%–60% of the Cu and Zn abundances. Exhalative-volcanic matter delivers a large fraction of Mn (78%–85%), some Fe (15%–21%), and possibly some Cu (38%–51%). Biogenous deposition is generally of restricted significance; at most 6%–35% of all Cu and Zn may derive from biogenic matter.

The exhalative-volcanic matter is slightly more abundant in the oldest deposits, reflecting a plate tectonic drift away from the volcanic Carlsberg Ridge. The Al/Ti ratio reveals that silicic crustal matter plays a somewhat larger role in the upper and lower part of the section studied, whereas the basaltic input is slightly higher in the intermediate levels (age 5–15 m.y.). The sediment abundances of Ba generally exceed those predicted by the models, an anomalous behavior also observed in equatorial Pacific sediments. This is possibly caused by poor knowledge of the input components.

Several changes in accumulation rates seem to correlate with climatic changes (onset of monsoon-driven upwellings and sea-level regressions of about 50–100 m at 10, 15–16, and 20–21 Ma). A number of constituents show higher accumulation rates at or shortly after these regressions, suggesting an accelerated removal of fines from shallow oceanic areas. Furthermore, the SiO_2/Al_2O_3 ratio shows a small increase in sediments younger than 10 Ma, implying an increase in biological productivity, particularly after the onset of monsoon-driven upwelling in the northwest Indian Ocean. This trend is paralleled by a general increase in the accumulation rates of Ba and $CaCO_3$. However, these accumulation rates are generally significantly lower than under the biological high-productivity zone in the equatorial Pacific. The onset of these upwelling systems about 10 Ma is probably related to the closing of the gap between India and the main Asiatic continent, preventing free circulation around the Indian subcontinent.

INTRODUCTION

Deep-sea sediments act as potential recorders of events on the continents and in the ocean, such as changes in climate, sea-level stand, plate tectonic processes, and deep-sea volcanism, provided that the sediments are well dated and that disruptions in the accumulation patterns, such as slumping or turbidite flows, can be identified. Site 711 (located at 02°44.56′S, 61°09.78′E, in a water depth of 4428 m; Backman, Duncan, et al., 1988) fulfills these requirements to a high degree. Furthermore, the site is located in an area where sediments should register variations in monsoon-driven upwelling, equatorial current systems, and associated biological productivity changes, as well as changing supply rates of lithogenic matter—processes that are at least partly controlled by the shifting plate tectonic setting of the northwest Indian Ocean, the closing of the Tethys Seaway, and the uplift of the Himalayas during the last 20 m.y. (Prell, Niitsuma, et al., 1989).

For these reasons, we decided to study the geochemistry of the uppermost 70 m of the sediment section at this site, since changes in constituents such as $CaCO_3$, excess silica (= opaline silica), Ba, Al, Ti, Zr, Ni, Cu, Zn, and Ba may indicate variations in biological productivity, as well as contributions from lithogenic constituents and exhalative-volcanic matter. Descriptions of the site and its geophysical characteristics, sampling procedures, and preliminary studies of the petrology macroscopic appearance, and chronology of these sediments have been reported elsewhere (Backman, Duncan, et al., 1988). Table 1 summarizes the sample distribution in Hole 711A as well as chronological, dry-bulk density, and accumulation rate data.

LABORATORY PROCEDURES

All sediments were dried at 100°C, weighed, and then heated to 1000°C to determine the loss on ignition (LOI). The samples were then mixed with lithium metaborite and fused at 1000°C for 30 min. The borate beads formed were subsequently dissolved in dilute nitric acid, after which the solutions were analyzed in an atomic emission spectrometer (AES) that uses inductively coupled argon plasma (ICP) as an excitation source; for further details, see Burman et al. (1978) and Burman and Boström (1979). Interlaboratory studies of the reference rock Ailsa Craig granite show the usefulness of these procedures (Boström, 1987).

Most analyses were made at the analytical division of SGAB (Swedish Geological Company), Luleå, but simultaneous checks of analytical precision and accuracy were made by ICP-AES on a similar unit at the Department of Geology, University of Stockholm (DGUS). Furthermore, some samples were supplied as unknown duplicates and others as unknown mixtures of various standard rocks and spectroscopically pure calcium carbonate ranging from 20% to 100% carbonate. These additional test procedures were run in parallel at SGAB and DGUS and show that the relative analytical errors generally are about 1%–2% for major elements such as silicon, aluminum, iron, calcium, and magnesium, and about 5%–10% for trace constituents such

[1] Duncan, R. A., Backman, J., Peterson, L. C., et al., 1990. *Proc. ODP, Sci. Results,* 115: College Station, TX (Ocean Drilling Program).

[2] Department of Geology, University of Stockholm, 106 91 Stockholm, Sweden.

Table 1. Basic data for Hole 711A.

Age (Ma)	Top and bottom cores and sections	Depth (mbsf)	*N*	Dry-bulk density (g/cm^3)	Accumulation rate (mg/cm^2/1000 yr)
0–1	1H-1, 1H-3	0–4.6	6	0.52	250
1–2	1H-5, 2H-1	4.6–9.6	7	0.59	280
2–3	2H-2, 2H-4	9.6–14.4	5	0.50	240
3–4	3H-1	14.4–19.2	2	0.40	190
4–5	3H-2, 3H-5	19.2–24.0	6	0.39	190
5–6	3H-7, 4H-1	24.0–28.8	5	0.45	220
6–7	4H-2, 4H-5	28.8–33.6	7	0.41	200
7–8	4H-5, 5H-1	33.6–38.4	6	0.70	340
8–9	5H-2, 5H-3	38.4–40.6	2	0.61	140
9–10	5H-3, 5H-4	40.6–42.2	2	0.61	100
10–11	5H-4	42.2–43.8	1	0.61	100
11–12	5H-5, 5H-6	43.8–45.4	3	0.81	130
12–13	5H-7, 6H-1	45.4–47.0	3	0.81	130
13–14	6H-1, 6H-2	47.0–48.6	2	0.81	130
14–15	6H-2, 6H-3	48.6–50.9	3	0.81	190
15–16	6H-4	50.9–53.7	1	0.81	230
16–17	6H-6, 6H-7	53.7–56.5	2	0.93	260
17–18	7H-1, 7H-2	56.5–59.3	3	0.58	160
18–19	7H-3, 7H-4	59.3–62.1	4	0.39	110
19–20	7H-5, 7H-6	62.1–64.9	3	0.61	170
20–21	7H-6, 8H-1	64.9–67.7	3	1.05	2.90
21–22	8H-2	67.7–70.5	3	0.90	250

Note: Age distributions in million years (m.y.) after Backman, Duncan, et al., 1988. Core and section numbering show top and bottom location of analyzed samples in each age interval studied. *N* = number of analyses used for the mean data presented in Table 2, 3, and 7. The accumulation rates (in mg/cm^2/1000 yr) are based on the dry-bulk densities and the sedimentation rates presented in Backman, Duncan, et al., 1988. The samples are identical to those used for the shipboard carbonate analyses for Cores 115-711A-1H to -8H (see Backman, Duncan, et al., 1988).

as copper, nickel, and zirconium. Aluminum, titanium, and zirconium data are particularly critical for the conservative mixing models discussed below; a test run including 17 identical sediment samples revealed relative analytical errors of 1%, 0.7%, and 8%, respectively, for these elements (Boström et al., in press).

All major elements were obtained as oxides, including CaO. The sum of oxides and the LOI were close to 100% (±1.5%), indicating that no major inorganic constituent was overlooked in the analytical work.

ANALYTICAL RESULTS AND PROCESSING OF DATA

The age intervals, core and section numbers, depth intervals, numbers of samples averaged, dry-bulk densities, and mass accumulation rates are shown in Table 1. Elemental abundances were averaged over 1-m.y. intervals; these mean values are presented in Table 2.

The $CaCO_3$ content was calculated, using data for CaO. These results show that large LOI values are primarily caused by the thermal breakdown of $CaCO_3$ at 1000°C, but a residual of about 8% LOI is obviously associated with the dehydration of clays and other sheet silicates, as data for the 8.5–13.5-m.y.-old sediments show (Table 2). Furthermore, some CaO is hosted in the weathered silicate fraction, the CaO/Al_2O_3 ratio probably being about 0.2. However, correcting for this small quantity of CaO in the lithogenous fraction has only marginally lowered the carbonate contents reported.

The $CaCO_3$ data in Table 2 agree well with direct measurements reported elsewhere in this volume. The carbonate content is generally negatively correlated with most other constituents (e.g., silica and alumina), as well as with the abundances of most trace elements, such as Cr, Cu, Ni, and V. These negative correlations indicate a significant carbonate dilution effect, except for the abundances of Sr. For this reason, the results were recalculated on a clay-matter basis. The sum of the major oxides is fairly constant in most pelagic sediments after carbonate, sea salt, organic matter, and excessive LOI have been removed (Landergren, 1964; Boström et al., 1972). A similar approach was used by Arrhenius (1966) and Schmitz (1987b).

The data in Table 2 indicate that most oxide sums (OS) approach 90% if the diluting carbonate is removed. Hence, using a factor *F*, defined as

$$F = \frac{90}{\text{OS(observed)}},$$

Table 2. Mean compositions of sediments, Hole 711A.

Mean age (Ma)	SiO_2 (%)	Al_2O_3 (%)	Fe_2O_3 (%)	MnO (%)	TiO_2 (%)	MgO (%)	K_2O (%)	Na_2O (%)	P_2O_5 (%)	$CaCO_3$ (%)	LOI (%)	Ba (ppm)	Co (ppm)
0.5	25.8	7.26	3.77	0.243	0.375	2.15	0.352	1.52	0.154	49.7	29.7	2390	12
1.5	30.7	8.73	4.68	0.310	0.467	2.77	0.531	2.04	0.204	39.3	26.3	3470	19
2.5	35.5	10.7	6.16	0.238	0.619	3.50	0.717	2.34	0.211	28.6	22.8	4150	22
3.5	46.5	14.1	8.23	0.462	0.879	4.76	2.12	4.48	0.358	4.04	13.7	3900	28
4.5	47.9	14.4	8.69	0.517	0.931	4.65	2.21	4.07	0.269	4.03	12.0	3390	33
5.5	45.3	13.2	7.85	0.334	0.834	4.49	1.72	3.63	0.302	10.0	15.1	3430	30
6.5	39.7	11.7	6.83	0.274	0.734	4.01	1.24	2.85	0.254	21.3	19.5	2810	30
7.5	35.5	10.9	6.36	0.199	0.659	3.58	0.989	2.06	0.225	30.2	21.5	2020	26
8.5	51.6	15.4	9.44	0.247	0.957	4.82	2.75	3.22	0.333	0.00	8.80	3060	26
9.5	51.5	16.0	9.99	0.574	1.03	4.26	2.71	2.95	0.307	0.00	8.45	3120	51
10.5	51.3	16.1	10.3	0.712	1.05	4.16	2.80	2.88	0.358	0.00	8.20	2400	65
11.5	51.1	16.1	10.3	0.670	1.05	4.21	2.81	2.90	0.379	0.00	8.33	2120	59
12.5	51.2	16.0	10.2	0.631	1.04	4.21	2.83	2.47	0.363	0.00	8.50	1890	51
13.5	51.8	16.4	10.1	0.429	0.989	4.35	3.00	2.76	0.343	0.00	8.45	910	43
14.5	37.6	12.0	6.90	0.378	0.695	3.72	1.57	1.67	0.240	27.3	19.4	780	34
15.5	51.6	16.3	10.3	0.597	0.971	4.42	3.07	2.73	0.321	0.00	8.40	910	53
16.5	47.8	15.3	10.0	0.694	0.897	3.86	2.64	2.46	0.415	6.39	10.9	980	50
17.5	50.5	15.8	11.2	0.819	0.932	3.92	2.77	2.71	0.459	0.42	8.67	1510	47
18.5	49.2	15.4	10.9	0.767	0.846	3.84	2.69	2.68	0.450	3.08	9.80	1530	42
19.5	48.8	15.2	10.2	0.643	0.807	3.77	2.55	2.66	0.401	5.15	10.8	1580	37
20.5	48.3	14.3	11.0	0.790	0.786	3.89	2.51	2.99	0.467	4.09	10.9	1890	43
21.5	11.1	2.97	2.77	0.098	0.142	1.09	0.085	0.333	0.171	78.3	37.4	1010	4.4

Note: Mean analytical results for sediment samples from Hole 711A. The sample distribution and number of analyses used for each mean calculation (= *N*) is given in Table 1. LOI = loss on ignition and ppm = parts per million.

one may recalculate all data in Table 2 to a clay-matter basis; the results are shown in Table 3 and Figure 1. Table 3 does not include data for MgO, Na_2O, K_2O, or Sr, as these constituents partly occur in interstitial water and carbonate phases.

This clay-normalization procedure is not without some problems, but it is less arbitrary than a simplistic recalculation on a carbonate-free basis, which may lead to very large errors. Thus, for sediments with 95% $CaCO_3$, 2.5% interstitial salt, and 0.5% organic matter, all reported clay-matter components are at least a factor 2.5 too low (Boström et al., 1972). For comparison, some other pelagic sediment analyses and sediment source components are presented, as well as some genetic mixing models (see Tables 4–6 and Figs. 2 and 3). Variations of the ratios of SiO_2, Fe_2O_3, MnO, and TiO_2 to Al_2O_3 with depth are shown in Figure 1.

Accumulation rates of the various components, calculated with the sedimentation rate and bulk density data in Table 1, are given in Table 7 and presented in Figures 4 and 5.

DISCUSSION

Compositional Variations of the Sediments

The data in Table 3 and Figure 1 indicate that the clay-matter-normalized abundances for SiO_2, Al_2O_3, Fe_2O_3, MnO, and TiO_2 vary only a little. Several trace constituents (Co, Cr, La, Sc, V, Y, Zr, Nb, and Yb) likewise show small variations (less than a factor of 3) between the extreme values; but Ba, Cu, Ni, and Zn show large variations (factors of about 6–10).

The high concentrations for silica and alumina and the low contents of manganese and most trace constituents strongly suggest that terrigenous matter is the major source of most of the sediment components. This impression is supported by data in Table 4, which show that the sediments at Site 711 have a marked geochemical similarity to sediment from the north central Pacific Ocean, a region that is dominated by a strong influx of terrigenous matter (Rex and Goldberg, 1958; Griffin and Goldberg, 1963. Arrhenius, 1966; Windom, 1975) but is poor in biogenous or exhalative-volcanic components (Boström, 1976; Boström et al., 1978). Thus, these North Pacific sediments and those of Site 711 are poor in trace constituents, as compared with pelagic sediments that occur in the equatorial Pacific, on the East Pacific Rise, and in the South Pacific (see Table 4). In view of its proximity to major land areas, the dominance of terrigenous matter at Site 711 is hardly surprising.

The Fe-Al and Mn-Al relations (Fig. 1) indicate that exhalative-volcanic matter may play a somewhat larger role, however, in the origin of the oldest sediments at Site 711, that is, when the site was closer to the spreading system on the Carlsberg Ridge. However, this volcanic influence is at best modest; only in the terrigenous-matter-dominated North Pacific sediments do we observe equally low Fe/Al and Mn/Al ratios (see Table 4). The SiO_2/Al_2O_3 and TiO_2/Al_2O_3 ratios (Fig. 1) suggest minor variations in the inputs of silicic and basic lithogenous components, with maximum inputs of basaltic matter occurring at 20–50 mbsf. A minimum in the barium abundances and a maximum in the chromium values (see Table 3) partly correlate with the TiO_2-Al_2O_3 distributions, which also suggests an increase in the basaltic component, as basaltic matter generally is poor in Ba and rich in Cr (see Table 5 and Krauskopf, 1979). However, the SiO_2/Al_2O_3 ratio is not a simple inverse of this relation but, rather, shows more silica in the top section (0–40 mbsf) than is to be expected from the basalt-granite mixtures that would produce the curve for TiO_2/Al_2O_3. This excess silica may represent biogenous silica and wind-borne quartz, and is primarily developed in sediments younger than 10 Ma.

This discussion shows that element ratios or enrichment factors (EF) may be indicative of the origin of a sediment. However, pelagic sediments have complex origins with several important input phases, including terrigenous matter (TM), biogenous matter (BM), and exhalative-volcanic matter (VM), all of which may contribute some silica and other constituents, but in varying proportions, as shown in Table 5. The element content E in a real sediment (RS) can therefore be described as a conservative mixture of the input phases, provided major losses do not occur after settling, for instance, as a result of redox processes. This condition is generally met by most well-oxidized pelagic sediments:

$$E_{RS} = f(aE_{BM} + bE_{VM} + cE_{TM}).$$

Table 2 (continued).

Cr (ppm)	Cu (ppm)	La (ppm)	Ni (ppm)	Sc (ppm)	Sr (ppm)	V (ppm)	Y (ppm)	Zn (ppm)	Zr (ppm)	Nb (ppm)	Yb (ppm)
48	18	23	22	11	886	61	32	37	74	7.7	3.1
54	20	27	56	13	763	71	41	46	91	9.3	3.8
56	17	38	143	16	696	83	49	67	127	16	4.8
92	21	62	99	22	269	112	73	34	172	25	6.2
83	61	55	146	22	257	116	60	42	182	27	5.3
71	27	54	143	21	386	98	65	22	160	22	5.8
67	11	44	135	18	572	85	54	43	139	17	4.9
76	10	39	129	16	697	80	47	77	121	14	7.4
121	37	56	39	23	165	123	68	63	175	23	6.3
110	122	54	127	23	168	134	63	74	182	29	6.0
100	49	61	35	22	159	139	72	85	183	29	6.6
106	96	58	93	22	153	140	70	76	182	27	6.5
113	146	57	151	22	149	143	67	84	173	25	6.4
207	219	54	190	22	122	146	63	100	163	24	6.0
87	59	37	152	15	654	98	44	85	121	15	4.2
105	284	60	195	21	126	132	63	104	203	26	6.0
93	228	57	175	20	274	130	68	78	168	24	6.3
93	211	63	140	21	161	143	74	122	165	24	6.7
89	156	63	126	19	23	130	74	113	172	25	6.7
79	80	61	114	17	274	120	69	100	228	36	6.6
75	64	70	92	17	241	124	79	73	219	36	7.2
13	19	19	8.9	3.9	1453	34	29	29	45	7	2.9

Table 3. Clay compositions of sediments, Hole 711A.

Mean age (Ma)	F	SiO_2 (%)	Al_2O_3 (%)	Fe_2O_3 (%)	MnO (%)	TiO_2 (%)	P_2O_5 (%)	Ba (ppm)	Co (ppm)	Cr (ppm)	Cu (ppm)
0.5	2.16	55.8	15.7	8.14	0.53	0.81	0.33	5170	27	104	38
1.5	1.78	54.8	15.6	8.35	0.55	0.83	0.36	6190	34	96	36
2.5	1.50	53.2	16.1	9.24	0.36	0.93	0.32	6230	33	83	26
3.5	1.10	51.1	15.5	9.06	0.51	0.97	0.39	4290	30	101	23
4.5	1.08	51.5	15.5	9.35	0.56	1.00	0.29	3650	36	89	65
5.5	1.16	52.5	15.3	9.10	0.39	0.97	0.35	3980	35	82	31
6.5	1.33	52.9	15.5	9.11	0.37	0.98	0.34	3750	40	89	14
7.5	1.49	52.8	16.3	9.46	0.30	0.98	0.33	3000	38	113	15
8.5	1.02	52.3	15.6	9.57	0.25	0.97	0.34	3100	26	123	38
9.5	1.01	51.9	16.1	10.1	0.58	1.04	0.31	3150	51	111	123
10.5	1.00	51.5	16.2	10.3	0.71	1.05	0.36	2410	65	100	49
11.5	1.01	51.4	16.2	10.3	0.67	1.05	0.38	2130	59	107	97
12.5	1.01	51.8	16.2	10.3	0.64	1.06	0.37	1910	52	114	148
13.5	1.00	51.7	16.3	10.1	0.43	0.99	0.34	919	42	207	219
14.5	1.39	52.3	16.7	9.58	0.53	0.97	0.33	1080	48	121	82
15.5	1.00	51.4	16.2	10.3	0.59	0.97	0.32	910	53	105	283
16.5	1.07	51.2	16.3	10.7	0.74	0.96	0.44	1050	53	100	245
17.5	1.01	51.0	16.0	11.3	0.83	0.94	0.46	1520	47	94	213
18.5	1.04	51.0	16.0	11.3	0.80	0.88	0.47	1590	44	93	162
19.5	1.06	51.7	16.1	10.8	0.68	0.85	0.42	1670	39	84	85
20.5	1.06	51.1	15.2	11.6	0.84	0.83	0.49	2000	46	80	68
21.5	4.81	53.2	14.3	13.4	0.47	0.68	0.82	4850	21	62	91

Note: Data from Table 2, recalculated on a clay-matter basis (i.e., by removing the diluting effects from carbonate, sea salts, organic matter, and other LOI constituents in the sediments). F = conversion factor used to obtain these values from those in Table 2; for details, see text.

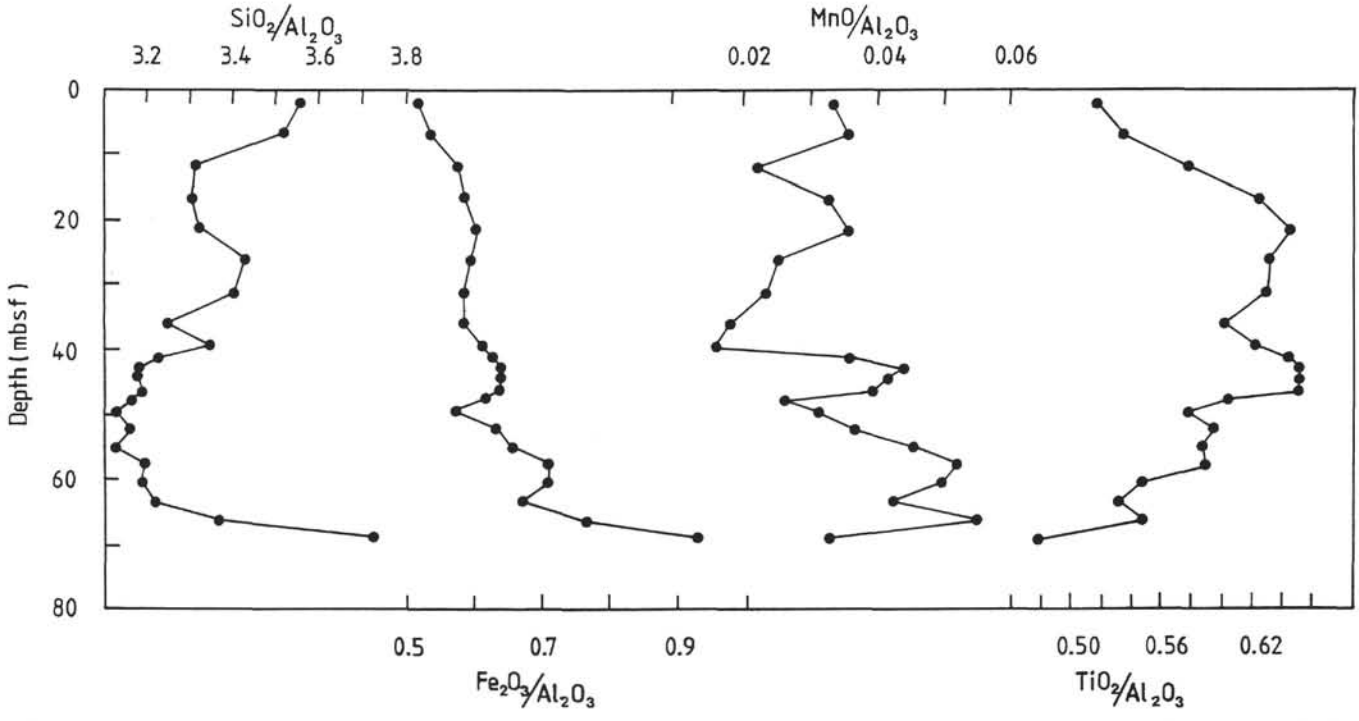

Figure 1. Variations in SiO_2/Al_2O_3, Fe_2O_3/Al_2O_3, MnO/Al_2O_3, and TiO_2/Al_2O_3 in sediments at Hole 711A, based on data in Table 2. Each dot represents the mean value for a 1-m.y. interval in the sediment.

In the above expression, a certain set of values for the coefficients *a, b,* and *c* yield the best-fit model for the real sediment, and minor shifts in the fits caused by small amounts of LOI are absorbed by the factor *f,* which never deviates much from 1.0. Even more complex models may be assumed (Boström et al., 1978).

This best-fit model approach makes it possible to test if a proposed explanation is correct. If a mixing model fails, then some aspects of the model must be poorly known, whereas discussions based on ratios or EF data generally lack this important feedback option. Ratio considerations may be misleading, therefore, when the relative roles of different input phases are studied in sediments of extreme types, but not necessarily always, as discussions of failing-ratio data show (Helz and Sinex, 1986).

Mixing models have been used in water studies (Andren et al., 1977; Boström et al., 1989), meteorite studies (Mason, 1962), and several sediment studies (Boström, 1976; Boström et al., 1976,

Table 3 (continued).

La (ppm)	Ni (ppm)	Sc (ppm)	V (ppm)	Y (ppm)	Zn (ppm)	Zr (ppm)	Nb (ppm)	Yb (ppm)	SiO_2/Al_2O_3	Fe_2O_3/Al_2O_3
50	47	23	132	70	80	160	17	6.8	3.56	0.519
48	99	23	127	74	83	162	16	6.7	3.52	0.536
56	215	24	125	74	101	191	24	7.1	3.31	0.575
68	109	24	124	80	38	189	28	6.8	3.31	0.586
59	157	23	125	64	45	196	29	5.7	3.32	0.602
62	166	24	114	75	25	185	26	6.7	3.43	0.595
59	180	24	113	72	58	185	23	6.5	3.41	0.587
57	191	24	118	70	114	179	20	11	3.25	0.582
57	39	23	125	68	63	178	23	6.3	3.35	0.613
55	128	23	136	63	74	184	29	6.1	3.23	0.626
61	35	22	140	72	85	184	29	6.6	3.19	0.640
58	94	22	141	71	76	183	27	6.5	3.18	0.639
58	152	23	145	68	85	175	26	6.4	3.19	0.636
53	189	22	145	63	100	163	24	6.0	3.17	0.618
52	211	21	137	61	119	169	21	5.9	3.13	0.575
60	194	21	132	63	104	202	26	6.0	3.17	0.632
62	188	21	139	73	84	180	25	6.8	3.13	0.657
64	141	21	144	75	123	167	24	6.8	3.20	0.709
65	131	20	137	76	117	178	26	7.0	3.19	0.709
65	121	18	127	73	106	241	38	7.0	3.22	0.672
74	97	18	131	83	77	232	38	7.6	3.37	0.767
92	43	19	163	138	138	218	34	13.8	3.72	0.935

Table 4. Mean compositions of various pelagic sediments.

Sediment	$CaCO_3$ (%)	SiO_2 (%)	Al_2O_3 (%)	Fe_2O_3 (%)	MnO (%)	TiO_2 (%)	Ba (ppm)	Cu (ppm)	Zn (ppm)	Ni (ppm)	V (ppm)	Zr (ppm)	Fe_2O_3/Al_2O_3	MnO/Al_2O_3
Hole 711A	14.2	52.2	15.8	10.1	0.56	0.94	2930	100	86	130	130	190	0.63	0.035
Indian Ocean Ridge	82.5	38.2	11.4	21.5	3.66	0.58	5110	520	—	380	270	200	1.87	0.32
Central Indian Ocean	30.6	50.8	12.8	10.4	2.24	0.72	1690	340	—	440	150	220	0.81	0.18
North Central Pacific	1.6	53	16.1	6.72	0.59	0.78	2900	300	—	150	130	150	0.42	0.037
South Central Pacific	36.8	44	13.0	10.7	2.19	0.93	3500	650	—	380	220	180	0.82	0.17
Equatorial Pacific	62.1	54	7.75	6.01	1.06	0.33	7700	420	—	160	82	110	0.78	0.14
East Pacific Rise	67.0	11.1	0.48	31.2	10.9	0.043	7200	1100	510	510	750	110	65	23

Note: Data for $CaCO_3$ represent absolute contents; other values correspond to clay-matter compositions. See also the discussion about data in Table 3. Hole 711A: mean data from this paper (Tables 2 and 3). Indian Ocean Ridge: mean data for five sediment cores from the area at 22°–27°S, 71°–77°E. Central Indian Ocean: mean data for four sediment cores from the area at 16°–20°S, 82°–90°E. North Central Pacific: mean data for sediments from the area at 6°–40°N, 150°E–120°W. South Central Pacific: mean data for sediments from the area at 10°–40°S, 120–170°W. Equatorial Pacific: mean data for sediments from the area at 6°N–10°S, 160°E–120°W. East Pacific Rise: mean data for sediments from the area at 10°–30°S, 100°–120°W. All data (except for Hole 711A) are derive from Boström (1976) and Boström (unpubl. data).

Table 5. Mean compositions of some sediment components.

Sediment component	SiO_2 (%)	Al_2O_3 (%)	Fe_2O_3 (%)	MnO (%)	TiO_2 (%)	Ba (ppm)	Cu (ppm)	Zn (ppm)	Ni (ppm)	V (ppm)	Zr (ppm)
Basaltic matter	49.2	15.9	12.3	0.22	1.5	20	80	100	85	250	110
Granitic matter	69.1	14.6	3.86	0.065	0.35	700	12	50	5	500	180
Tarrigenous matter	53.3	15.3	7.01	0.114	0.80	540	57	78	90	130	190
Biogenous matter	17.4	0.53	0.69	0.019	0.062	480	280	890	93	21	24
Volcanic-exhalative matter	3.69	0.16	10.4	3.62	0.014	2400	380	170	170	250	37

Note: Mean compositions are based on data in Krauskopf (1979) and Boström et al. (1978).

1978, 1979, 1989; Bischoff et al., 1979). We find such modeling superior to the commonly used factor analysis, which often produces results that are hard to translate into concrete physical models, and which must be interpreted by means of known element abundances in potential input phases to solve the provenance problems.

Mixing models for various examples of pelagic sediments in Table 4 are presented in Figure 2, whereas Figure 3 shows models for some sediments from Site 711. In these models, the concentrations (in %) are given in logarithmic units; and the total real sediment compositions have been used (i.e., we did not correct for dilution effects on the element abundances). $CaCO_3$ presents a special problem, however, in view of its selective dissolution under the calcite compensation depth (CCD) and because of the selective shedding of calcite exoskeletons by planktonic organisms. For that reason, Ca data are not used in the modeling (see Table 5).

A total of 66 models were obtained by mixing TM, BM, and VM in 10% increments in all possible permutations. The models were subsequently tested for fit between the models and the real sediments. The results presented in Figure 2 corroborate previous findings that sediments from the central parts of the Indian and Pacific oceans contain much biogenous matter (Boström, 1976; Boström et al., 1978). For the modeling of the Site 711 sediments, a further refinement was performed close to the best-fit models obtained by also using input increments of 5%–

Table 6. Provenance models for pelagic sediments.

Constituent	Model central Indian Ocean 0.4BM + 0.2 VM + 0.4 TM			Model south central Pacific 0.4 BM + 0.3 VM + 0.3 TM			Model equatorial Pacific 0.8 BM + 0.1 VM + 0.1 TM			Model Hole 711A sediments 0.05–0.025 BM + 0.10–0.15 VM + 0.825–0.85 TM		
	BM	VM	TM	BM	VM	TM	BM	VM	TM	BM	VM	TM
SiO_2	25	2	73	29	5	66	71	2	27	1–2	0.8–1.2	98–99
Al_2O_3	4	0.5	96	4	1	95	21	0.8	78	0.1–0.2	0.1–0.2	99–100
Fe_2O_3	6	40	54	5	57	38	23	46	31	0.2–0.5	15–21	79–85
MnO	1	93	6	1	96	3	4	93	3	0.1–0.2	78–85	15–21
TiO_2	7	0.8	92	9	2	89	37	1	61	0.2–0.5	0.2–0.3	99
Ba	22	54	24	18	67	15	57	35	8	(7)	(33)	(60)
Cu	53	36	11	46	47	7	84	14	2	6–14	38–51	42–48
Zn	85	8	7	81	12	5	97	2	1	20–35	13–23	52–57
Ni	34	32	34	33	44	23	74	17	9	2–5	17–25	73–78
V	8	45	47	7	61	32	30	46	24	0.4–0.8	18–26	74–81
Zr	10	8	82	13	14	73	46	9	45	0.4–0.7	2–3	96–97

Note: Fractions of sediments (in %) explained by the provenance models. See also plots of best fits in Figures 2A–2C and 3A–3C.

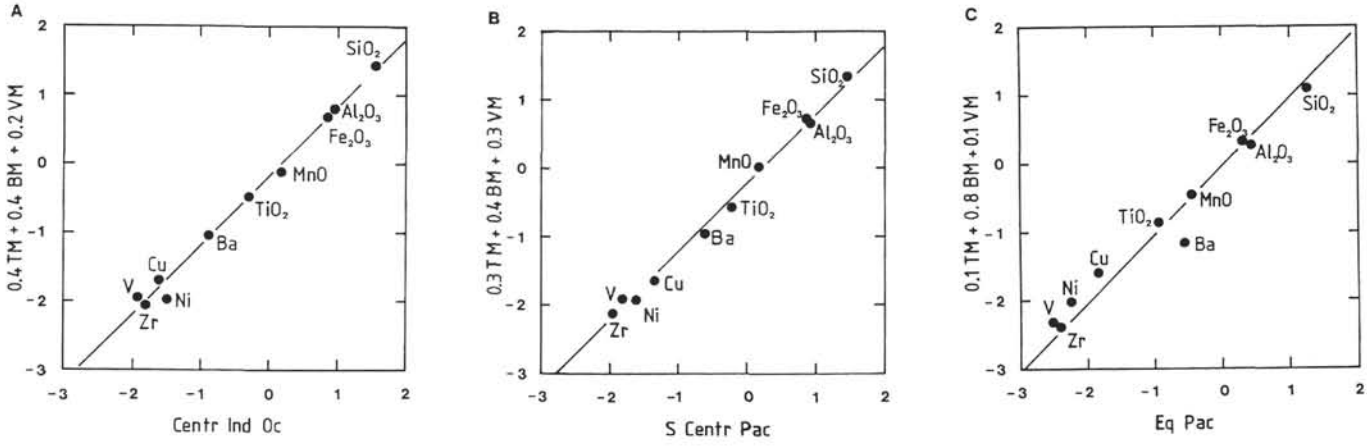

Figure 2. Comparisons between real sediments (various pelagic deposits) and model sediments, obtained by mixing the input components TM, VM, and BM (see Tables 4 and 5). All concentrations given in percentages on a logarithmic basis. **A.** Central Indian Ocean sediment. **B.** South Central Pacific sediment. **C.** Equatorial Pacific sediment.

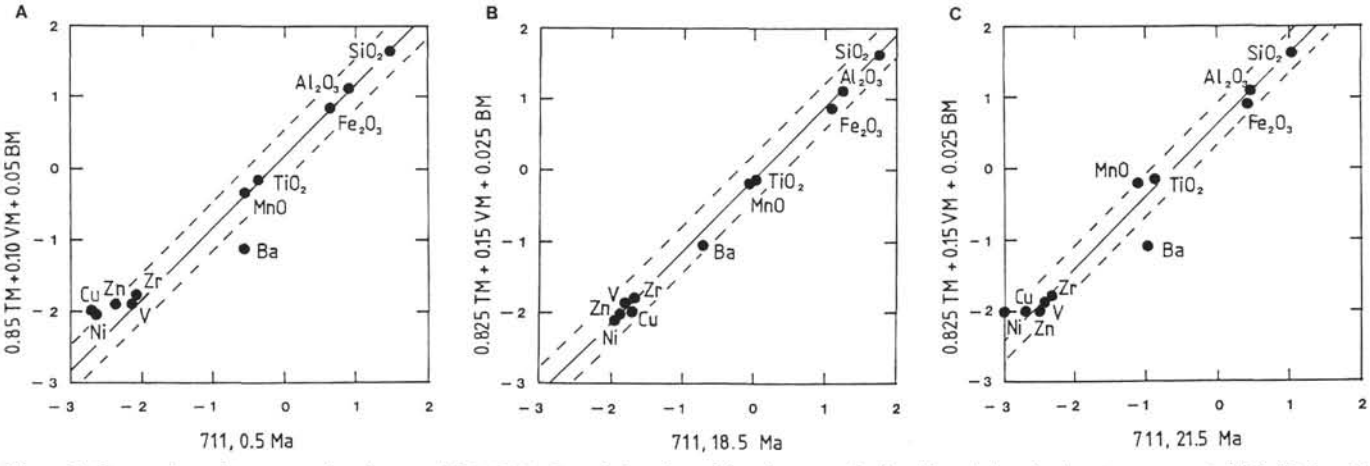

Figure 3. Comparisons between real sediments (Hole 711A deposits) and model sediments, obtained by mixing the input components TM, VM, and BM (see Tables 4 and 5). All concentrations are given in percentages on a logarithmic basis. **A.** Hole 711A (0.5 Ma). **B.** Hole 711A (18.5 Ma). **C.** Hole 711A (21.5 Ma).

Table 7. Accumulations rates for sediments from Hole 711A.

Mean age (Ma)	$CaCO_3$	SiO_2	Al_2O_3	Fe_2O_3	MnO	TiO_2	MgO	P_2O_5	Ba	Co	Cr	Cu	La	Ni	Sc	Sr	V	Y	Zn	Zr	Nb	Yb
	(mg/cm^2/1000 yr)								(mg/cm2/1,000,000 yr)													
0.5	124	65	18	9.4	0.61	0.94	5.4	0.39	598	3.1	12	4.4	5.7	5.4	2.7	221	15	8.1	9.3	19	1.9	0.78
1.5	110	86	24	13	0.87	1.3	7.8	0.57	972	5.3	15	5.7	7.5	16	3.6	214	20	12	13	26	2.6	1.1
2.5	69	85	26	15	0.57	1.5	8.4	0.51	996	5.3	13	4.1	9	34	3.8	167	20	12	16	31	3.9	1.1
3.5	7.7	55	27	16	0.88	1.7	9.0	0.68	741	5.2	18	4.0	12	19	4.2	51	21	14	6.6	33	4.8	1.2
4.5	7.7	91	27	17	0.98	1.8	8.8	0.51	644	6.3	16	12	11	28	4.1	49	22	11	8.0	35	5.2	1.0
5.5	22	100	29	17	0.74	1.8	9.9	0.66	755	6.6	16	5.9	12	32	4.5	85	22	14	4.8	35	4.9	1.3
6.5	43	79	23	14	0.55	1.5	8.0	0.51	562	6.0	13	2.1	8.9	27	3.5	114	17	11	8.7	28	3.4	0.98
7.5	103	121	37	22	0.68	2.2	12	0.77	687	8.7	26	3.4	13	44	5.4	237	27	16	26	41	4.7	2.5
8.5	0	72	22	13	0.35	1.3	6.7	0.47	428	3.6	17	5.3	7.8	5.4	3.2	23	17	9.5	8.8	25	3.1	0.88
9.5	0	51	16	10	0.57	1.0	4.3	0.31	312	5.1	11	12	5.4	13	2.3	17	13	6.3	7.4	18	2.9	0.60
10.5	0	51	16	10	0.71	1.1	4.2	0.36	240	6.5	10	4.9	6.1	3.5	2.2	16	14	7.2	8.5	18	2.9	0.66
11.5	0	66	21	13	0.87	1.4	5.5	0.49	276	7.7	14	13	7.5	12	2.9	20	18	9.1	9.8	24	3.5	0.84
12.5	0	67	21	13	0.82	1.4	5.5	0.47	246	6.6	15	19	7.4	20	2.9	19	19	8.7	11	23	3.3	0.83
13.5	0	67	21	13	0.56	1.3	5.7	0.45	118	5.5	27	29	7.0	25	2.9	16	19	8.2	13	21	3.1	0.78
14.5	52	71	23	13	0.72	1.3	7.1	0.46	148	6.5	17	11	7.1	29	2.9	124	19	8.4	16	23	2.9	0.80
15.5	0	119	37	24	1.4	2.2	10	0.74	209	12	24	65	14	45	4.8	29	30	15	24	47	6.0	1.4
16.5	17	124	40	26	1.8	2.3	10	1.1	255	13	24	59	15	46	5.2	71	34	18	20	44	6.1	1.6
17.5	0.67	81	25	18	1.3	1.5	6.3	0.73	242	7.5	15	34	10	22	3.3	26	23	12	20	26	3.8	1.1
18.5	3.4	54	17	12	0.84	0.93	4.2	0.50	168	4.6	9.8	17	6.9	14	2.1	25	15	8.1	12	19	2.7	0.74
19.5	8.8	83	26	17	1.1	1.4	6.4	0.68	269	6.3	14	14	10	19	2.9	47	21	12	17	39	6.1	1.1
20.5	12	140	42	32	2.3	2.3	11	1.4	548	13	22	19	20	27	4.9	70	36	23	21	64	11	2.1
21.5	196	28	7.4	6.9	0.25	0.36	2.7	0.43	253	1.1	3.2	4.8	4.8	2.2	1.0	363	8.5	7.2	7.2	11	1.8	0.72

Note Accumulation rates for sediments at Hole 711A, derived from data in Tables 1 and 2 (this chapter).

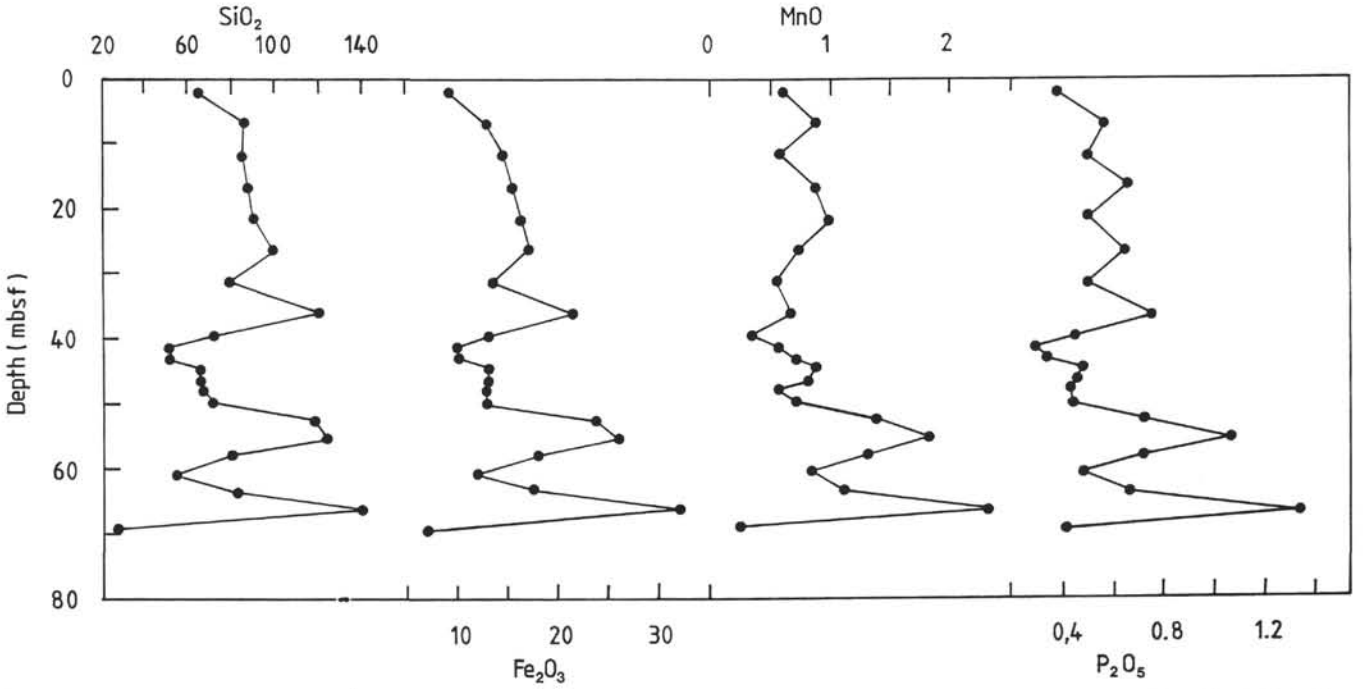

Figure 4. Accumulation rates (mg/cm^2/1000 yr) for SiO_2, Fe_2O_3, MnO, and P_2O_5 in sediments at Hole 711A, based on data in Table 7. Each dot represents the mean value for a 1-m.y. sedimentation interval. Note maxima at 7.5, 16.5, and 20.5 Ma, and minima at 6.5, 9.5–10.5, and 18.5 Ma. Accumulation rate patterns for Al_2O_3, TiO_2, and Zr resemble that for SiO_2, whereas accumulation rate variations for V and Co resemble that for Fe_2O_3. The rare-earth-elements La, Y, and Yb have accumulation rates that covary with those for P_2O_5.

2.5% in six cases. The best-fit models in Figure 3 show correlations vs. the real sediments of 0.979–0.998; other models for these real sediments show correlations that are distinctly poorer. However, the fit of models similar to the best-fit models is rather insensitive to variations of 5%–2.5% in the mixing constituents. A repetition of these modeling procedures using (1) only data for Si, Al, Fe, Mn, and Ti and (2) only data for Ba, Cu, Zn, Zr, Ni, and V yielded the same results.

The graphs in Figure 3 demonstrate that the models explain the origins of the sediments to a high degree, most model abundances agreeing with sediment abundances to ±15% or better, the exception being Ba in some cases. By means of the best-fit proportions of the input components and their compositions, one can calculate the fraction of a given component that derives from TM, BM, or VM (see Table 6). These results show that terrigenous matter is the main supplier of Al, Ti, and Zr in most

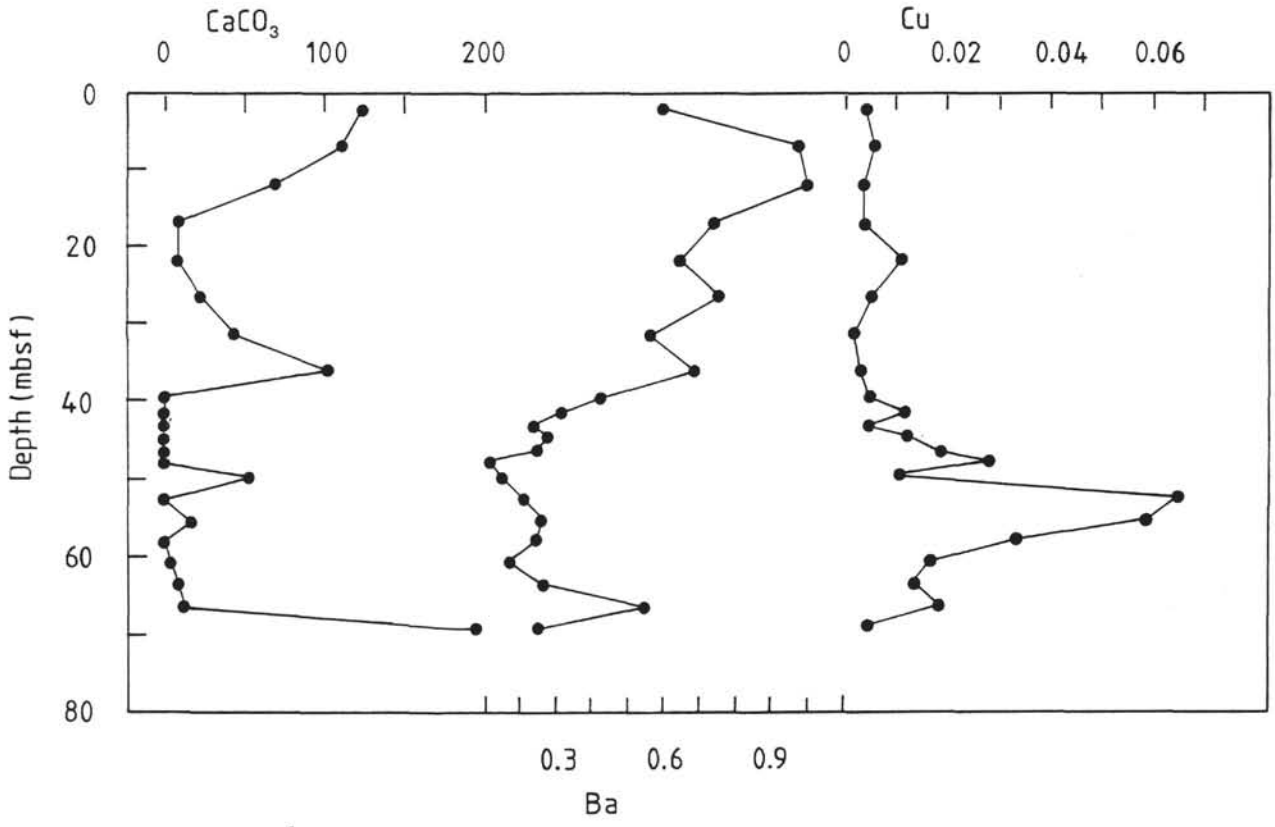

Figure 5. Accumulation rates (mg/cm^2/1000 yr) for $CaCO_3$, Ba, and Cu in sediments at Hole 711A; for details, see caption to Figure 4. Accumulation rates for Sr covary with those for $CaCO_3$, whereas the accumulation rates for Ba and Cu are rather unique. Note that the spikes at 7.5, 16.5, and 18.5 Ma are only partly present for $CaCO_3$, Ba, and Cu.

models. However, BM contains clearly measurable quantities of these elements (Arrhenius, 1963; Martin and Knauer, 1973; Turekian et al., 1973; Bryan, 1976; Boström et al., 1978; Förstner and Wittmann, 1981; Knauss and Ku, 1983; Collier and Edmond, 1984). In sediments from the equatorial Pacific Ocean high-productivity zone, 20%–45% of these elements may be of a biological origin.

The TM explains most of the Si, Al, Ti, and Zr abundances (96%–100%); about 73%–85% of all Fe, V, and Ni; and 40%–60% of all Cu and Zn. BM is a significant source only for zinc and copper (6%–35%). About 78%–85% of all Mn derives from VM, whereas only 15%–21% of all Fe and 15%–50% of all Cu, Ni, and V have this origin. These results corroborate the impression that both Site 711 and central North Pacific sediments are largely controlled by terrigenous contributions; only for manganese, copper, and zinc are VM and BM critical in the models. This does not exclude the fact that some minor variations in the distribution of various constituents are caused by changes in the relative roles of the source components.

The plots in Figures 2 and 3, as well as the results of Boström (1976) and Boström et al. (1978), show that Ba sometimes does not fit well into these conservative models, particularly for sediments in high-productivity areas (Fig. 2C). This is probably because of an oversimplified choice of biological matter, a problem approached by Brongersma-Sanders (1966), who considered the possibility that diatoms were selectively enriched in and transporting Ba to the ocean floor. Too few analyses of bulk planktonic samples with a wide geographical distribution exist at present to test this hypothesis more thoroughly, but the interpretation is supported by the widely occurring correlation between opaline silica and barium in many sediments (Goldberg and Arrhenius, 1958; Boström et al., 1973a, 1979; Gurvich et al., 1978; Schmitz, 1987b).

It is still far from clear which planktonic organisms play the major role in the transport of Ba and other trace elements to the deep-sea floor, and in what form this transport takes place (Martin, 1970; Turekian and Chan, 1971; Higgo et al, 1977); a review of the subject is presented in Schmitz (1987b). In some cases, the correlation between opaline silica and barium is poor or even negative; for example, where volcanic contributions are large. Similar conclusions can be drawn from evidence presented by Lizitsin (1966), Boström et al. (1973b, 1979), and Schmitz (1987b).

At Site 711, the sediments show the highest Ba concentrations (3000–6200 ppm) and silica/alumina ratios (3.23/3.56) in the youngest sediments (0–10 Ma), whereas with few exceptions all older sediments show lower values (see Table 3). This suggests a correlation between an opaline silica phase and Ba. The opaline silica is easily identified under the microscope high up in the sequence (Backman, Duncan, et al., 1988), but the massive deposition of TM obscures the exact onset of opaline silica deposition at this site.

Accumulation Rates

Accumulation rates for sediments at Site 711 are shown in Table 7 and in Figures 4 and 5, and for other Pleistocene sediments in Table 8. These tables indicate that Site 711 sediments and those from the central North Pacific are very similar, except for Cu.

Table 8. Accumulation rates for some Pleistocene pelagic sediments.

	North Central Pacific	Equatorial Pacific	South Central Pacific	Hole 711A
Opalaline SiO_2	3–20	20–150	3–20	ND (small)
Total SiO_2	12–200	30–330	9–56	75
Al_2O_3	3–60	3–60	2–12	21
Fe_2O_3	6–15	10–30	≈6	11
MnO	≈1	1–4	≈1	0.75
Ba	0.1–1.0	0.2–4.0	0.1–1.0	0.80
Cu	0.01–0.04	0.03–0.15	0.025–0.05	0.0055

Note: Accumulation rates, in $mg/cm^2/1000$ yr, for Pleistocene pelagic sediments, based on data in Table 7 (this chapter) and Boström et al. (1973a, 1973b). ND = not determined.

Variations in the accumulation rates of several major and trace components reveal several events of interest. For example, distinct accumulation rate maxima occur at 7.5, 16.5, and 20.5 Ma, and minima at 6.5, 9.5–10.5, and 18.5 Ma (Table 7 and Fig. 4). With some minor variations, this pattern is shown by SiO_2, Al_2O_3, TiO_2, Zr, Fe_2O_3, V, Co, P_2O_5, and the rare-earth-elements La, Y, and Yb. Manganese oxide has a poorly developed 7.5-Ma spike (see Fig. 3), but otherwise its accumulation rate pattern resembles that of most major components. Very different accumulation rate patterns (Fig. 5 and Table 7) are shown by $CaCO_3$ and Sr, and by Ba and Cu, with the last two patterns lacking all similarities to those of any other constituent.

The covarying but fluctuating accumulation rates for the lithogenous components contrast with the restricted compositional variations shown in Table 3, suggesting that the lithogenous phase is of fairly constant composition but is deposited at irregular rates. Studies of Pleistocene sediments in the Atlantic Ocean reveal distinct correlations with the regressions and transgressions that are associated with glacial and interglacial events (Wangersky and Hutchinson, 1958; Boström, 1970; Boström and Fisher, 1972). Upward migration in the sediments of mobile components has also been suggested as a cause for changes in the accumulating sediments (Bonatti et al., 1971). However, in the present case, migration can be ruled out because of the refractory nature of Al, Ti, and Zr.

Sea-level reconstructions by Haq et al. (1987) indicate that major regressions took place at about 20–21, 15–16, and 10 Ma. The two oldest and also strongest spikes in Figure 3 coincide with these events, but the youngest pulse at 7.5 Ma shows a lag of about 2.5 m.y., which is rather large to make a regression the likely cause.

Studies in the eastern Indian Ocean and of Bengal Fan sediments reveal that sedimentation patterns changed rather drastically about 10 Ma, reflecting the uplift and beginning erosion of the Himalayas (Schmitz, 1987a). As a consequence, one should expect to see a record of similar events in the northwest Indian Ocean, which receives terrigenous sediments from the Indus River. We find it noteworthy that after about 9 Ma the accumulation rates in this part of the Indian Ocean (see Fig. 4) show smaller fluctuations than in the age interval from 21.5 to 9.5 Ma. Although the Indus Valley most certainly did not supply coarse matter to Site 711, the large mud loads coming down the Indus River may nevertheless have added to the suspended matter loads that could drift far out to sea. Another, and perhaps still more important, source of material was the onset of the monsoon wind systems, which probably started at this time (Leg 117 Scientific Drilling Party, 1988a, 1988b; Prell, Niitsuma, et al., 1989) and which could transport eolian matter considerable distances, as is the case even today.

Simultaneous with the onset of the monsoon wind system, the monsoon-driven upwelling systems were developed in the northwest Indian Ocean (Leg 117 Scientific Drilling Party, 1988a, 1988b). As a consequence, biological productivity increased considerably, which is reflected in high accumulation rates for $CaCO_3$, Ba (see Fig. 5), and opaline silica (Backman, Duncan, et al., 1988). It does not appear likely, however, that this productivity increase was an exclusive result of the start-up of a monsoon system. During the early stage of its northward drift, the Indian subcontinent was surrounded by oceanic waters on all sides, and the Tethys Seaway was still open toward the west (Davies and Kidd, 1977; Sclater et al., 1977). Hence, upwelling phenomena might not have been very strong at that time, even if monsoon-wind systems did exist, because many current systems could resupply the surface waters moved around by the winds. After the Indus Passage north of India and the Tethys Seaway closed, the whole Arabian Sea turned into a large cul-de-sac, in which upwelling processes were probably established more easily.

The accumulation rate pattern for copper shows a sixfold increase in accumulation rate in the sediments at 15.5–16.5 Ma compared with all other sediments (see Fig. 5). This spike correlates well with similar peaks for most major and trace components like SiO_2, Fe_2O_3, MnO, P_2O_5, Co, Cr, and Ni. The remaining Cu accumulation rate pattern shows no significant similarity with that of any other element. Copper is often correlated with Mn (Boström, 1970), but not in the present case.

One possible scenario is that the sediments at Site 711 did not accumulate under well-oxidizing conditions, so that minor postdepositional redox processes may have caused some trace element migration in the sediments (e.g., of copper and zinc). However, the overall accumulation rates are not particularly high, as shown in Table 8; even sediments from the open equatorial Pacific far from the continents show considerably higher accumulation rates (Boström et al., 1979). This suggests that the overall effects of the biological input are comparatively weak, which is corroborated by the fact that most of the geochemical variations described above tend to be poorly developed. This enigmatic situation is probably because Site 711 is located too far from the area of most intense eolian deposition to register the monsoon effects well.

Carbonate accumulation curves are studied in detail elsewhere (Peterson and Backman, this volume) in conjunction with a discussion of the variations of the carbonate compensation depth in the northwest Indian Ocean during geological time.

CONCLUSIONS

The noncarbonate fraction of the sediments at Site 711 (0–22 Ma) consist primarily of terrigenous components that are poor in oxidized phases and biogenous components, as indicated by the relatively low Mn, Ba, Cu, Zn, and Ni abundances. Accumulation rates and compositional variations of the sediments from Hole 711A are similar to those found in deposits from the north central Pacific. It appears that Site 711 is located too far from the area of distinctly monsoon-controlled processes to be ideal for monitoring the waning and waxing of the monsoon processes.

ACKNOWLEDGMENTS

We want to thank the ODP curators for making required samples available for these studies. We also want to thank C. Pontér, SGAB, and B. Boström for assistance with and discussion of analytical methods and results. This project was supported by grants from the Swedish Natural Sciences Research Council (NFR); this support is gratefully acknowledged.

REFERENCES

Andren, A. W., and Lindberg, S. E., 1977. Atmospheric input and origin of selected elements in Walker Branch watershed, Oak Ridge, Tennessee. *Water, Air, Soil Pollut.,* 8:199–215.

Arrhenius, G., 1963. Pelagic sediments. *In* Hill, M. N. (Ed.), *The Sea* (Vol. 3): *The Earth Beneath the Sea: History:* New York (Wiley-Interscience), 655–727.

_____, 1966. Sedimentary record of long-period phenomena. *In* Hurley, P. M. (Ed.), *Advances in Earth Science:* Cambridge, MA (M.I.T. Press), 155–174.

Backman, J., Duncan, R. A., et al., 1988. *Proc. ODP, Init. Repts,* 115: College Station, TX (Ocean Drilling Program).

Bischoff, J. L., Piper, D. Z., and Quintero, P., 1979. Nature and origin of metalliferous sediments in Dome Site C, Pacific manganese nodule province. *In* Lalou, C. (Ed.), *La Genese des nodules de manganese.* Colloq. Int. CNRS, 289:119–138.

Bonatti, E., Fisher, D. E., Joensuu, O., and Rydell, H. S., 1971. Postdepositional mobility of some transition elements, phosphorus, uranium and thorium in deep-sea sediments. *Geochim. Cosmochim. Acta,* 35:189–201.

Boström, B., 1987. Report on Ailsa Craig Granite. *In* Govindaraju, K. (Ed.), Compilation Report on Ailsa Craig Granite AC-E with the Participation of 128 GIT-IWG Laboratories. *Geostand. Newsl.,* 11: 203–255.

Boström, K. 1970. Deposition of manganese-rich sediments during glacial periods. *Nature,* 226:629–630.

_____, 1976. Particulate and dissolved matter as sources for pelagic sediments. *Stockholm Contrib. Geol.,* 30:15–79.

Boström, K., Boström, B., and Andersson, P., 1989. Natural and anthropogenic components in bulk precipitation at Blidö (Archipelago of Stockholm). *Water Resources Res.,* 25:1291–1301.

Boström, K., and Fisher, D. E., 1972. Lateral fluctuations in pelagic sedimentation during the Pleistocene glaciations. *Boreas,* 1:275–288.

Boström, K., Joensuu, D., Moore, C., Boström, B., Dalziel, M,, and Horowitz, A., 1973b. Geochemistry of barium in pelagic sediments. *Lithos,* 6:159–174.

Boström, K., Joensuu, O., Valdés, S., Charm, W., and Glaccum, R., 1976. Geochemistry and origin of East Pacific sediments sampled during DSDP Leg 34. *In* Yeats, R. S., Hart, S. R., et al., *Init. Repts. DSDP,* 34: Washington (U.S. Govt. Printing Office), 556–574.

Boström, K., Joensuu, O., Valdés, S., and Riera, M., 1972. Geochemical history of South Atlantic Ocean sediments since Late Cretaceous. *Mar. Geol.,* 12:85–121.

Boström, K., Kraemer, T., and Gardner, S., 1973a. Provenance and accumulation rates of opaline silica, Al, Ti, Fe, Mn, Cu, Ni, and Co in Pacific pelagic sediments. *Chem. Geol.,* 11:123–148.

Boström, K., Lysén, L., and Moore, C., 1978. Biological matter as a source of authigenic matter in pelagic sediments. *Chem. Geol.,* 23: 11–20.

Boström, K., Moore, C., and Joensuu, O., 1979. Biological matter as a source for Cenozoic deep sea sediments in the equatorial Pacific. *Ambio, Spec. Rep.,* 6:11–17.

Boström, K., Perissoratis, C., Galanopoulos, V., Papavassiliou, C., Boström, B., Ingri, I., and Kalogeropoulos, S., in press. Geochemistry and structural control of hydrothermal sediments in the Caldera of Santorini, Greece. *Thera and the Aegean World* (Vol. III).

Brongersma-Sanders, M., 1966. Barium in pelagic sediments and in diatoms. *Proc. K. Ned. Akad. Wet., Ser. B: Palaeontol., Geol., Phys., Chem., Anthropol.,* 70:93–99.

Bryan, G. W., 1976. Heavy metal contamination in the sea. *In* Johnston, R. (Ed), *Marine Pollution:* London (Academic Press), 185–302.

Burman, J. O., and Boström, K., 1979. Comparison of different plasma excitation and calibration methods in the analyses of geological materials by optical emission spectrometry. *Anal. Chem.,* 51:516–520.

Burman, J. O., Pontér, C., and Boström, K., 1978. Metaborite digestion procedure for inductively coupled plasma-optical emission spectrometry. *Anal. Chem.,* 50:679–680.

Collier, R., and Edmond, J., 1984. The trace element geochemistry of marine biogenic particulate matter. *Prog. Oceanogr.,*13:113–199.

Davies, T. A., and Kidd, R. B. 1977. Sedimentation in the Indian Ocean through time. *In* Heirtzler, J. R., Bolli, H. M., Davies, T. A., Saunders, J. B., and Sclater, J. G. (Eds.), *Indian Ocean Geology and Biostratigraphy:* Washington (American Geophysical Union), 61–85.

Förstner, U., and Wittmann, G.T.W., 1981. *Metal Pollution in the Aquatic Environment* (2nd ed.): Berlin-Heidelberg-New York (Springer-Verlag).

Goldberg, E. D., and Arrhenius, G., 1958. Chemistry of Pacific pelagic sediments. *Geochim. Cosmochim. Acta,* 13:153–212.

Griffin, J. J., and Goldberg, E. D., 1963. Clay mineral distribution in the Pacific ocean. *In* Hill, M. N. (Ed.), *The Sea* (Vol. 3): *The Earth Beneath the Sea: History:* New York (Wiley-Interscience), 728–741.

Gurvich, Y. G., Bogdanov, Y. A., and Lisitzin, A. P., 1978. Behavior of barium in recent sedimentation in the Pacific. *Geochem. Int.,* 15: 28–43.

Haq, B, U., Hardenbol, J., and Vail, P. R., 1987. Chronology of fluctuating sea levels since the Triassic. *Science,* 235:1156–1167.

Helz, G. R., and Sinex, S. A., 1986. Influence of infrequent floods on the trace metal composition of estuarine sediments. *Mar. Chem.*, 20: 1–11.

Higgo, J.J.W., Cherry, R. D., Heyraud, M., and Fowler, S. W., 1977. Rapid removal of plutonium from the oceanic surface layer by zooplankton faecal pellets. *Nature,* 266:623–624.

Krauskopf, K. B., 1979. *Introduction to Geochemistry* (2nd ed): New York (McGraw-Hill).

Knauss, K., and Ku, T. L., 1983. The elemental composition and decay series radio nuclide content of plankton from the East Pacific. *Chem. Geol.,* 39:125–145.

Landergren, S., 1964. On the geochemistry of deep-sea sediments. *Rep. Swed. Deep-Sea Exped. X, Spec. Investig.,* No. 5, Göteborg.

Leg 117 Scientific Drilling Party, 1988a. Leg 117 finds mountains, monsoons. *Geotimes,* 33(3):1–16.

Leg 117 Shipboard Scientific Party, 1988b. Milankovitch and monsoons. *Nature* 331:663–664.

Lisitzin, A. P., 1966. Main regularities in the distribution of recent siliceous sediments and their relations with climatic zonality (in Russian; English table of contents). *Geokhim. Kremnezema* (Geochemistry of Silica): Moscow (Akademia Nauka SSSR), 90–191.

Martin, J. H., 1970. The possible transport of trace metals via moulted copepod exoskeletons. *Limnol. Oceanogr.,* 15:756–776.

Martin, J. H., and Knauer, G. A., 1973. The elemental compositions of plankton. *Geochim. Cosmochim. Acta,* 37:1639–1653.

Mason, B., 1962. *Meteorites:* New York (Wiley and Sons).

Prell, W. L., Niitsuma, N., et al., 1989. Introduction, background, and major objectives for ODP Leg 117. *Proc. ODP., Init. Repts.,* 117: College Station, TX (Ocean Drilling Program).

Rex, R. W., and Goldberg, E. D.,1958. Quartz contents of pelagic sediments of the Pacific Ocean. *Tellus,* 10:153–159,

Schmitz, B., 1987a. The TiO_2/Al_2O_3 ratio in the Cenozoic Bengal Abyssal Fan sediments and its use as a paleostream energy indicator. *Mar. Geol.,* 76:195–206.

_____, 1987b. Barium, equatorial high productivity and the northward wandering of the Indian continent. *Paleoceanography,* 2:63–77.

Sclater, J. G., Abbott, D., and Thiede, J., 1977. Paleobathymetry and sediments of the Indian Ocean. *In* Heirtzler, J. R., Bolli, H. M., Davies, T. A., Saunders, J. B., and Sclater, J. G. (Eds.), *Indian Ocean Geology and Biostratigraphy:* Washington (American Geophysical Union), 25–59.

Turekian, K. K., and Chan, L. H., 1971. The possible role of iron oxide in determining the trace element composition of calcareous tests. *AEC, Annu. Progr. Rep.,* F1-F4.

Turekian, K. K., Katz., A., and Chan, L., 1973. Trace element trapping in pteropod tests. *Limnol. Oceanogr.,* 18:240–249.

Wangersky, P. J., and Hutchinson, G. E., 1958. Manganese deposition and deep water movements in the Caribbean. *Nature,* 181:108–109.

Windom, H. L., 1975. Eolian contributions to marine sediments. *J. Sediment. Petrol.,* 45:520–529.

Date of initial receipt: 2 June 1989
Date of acceptance: 11 January 1990
Ms 115B-182